ACS APPLIED MATERIALS & INTERFACES

Research Article

www.acsami.org

Production of Biocompatible and Antimicrobial Bacterial Cellulose Polymers Functionalized by RGDC Grafting Groups and Gentamicin

Mahmoud Rouabhia,*[,†] Jérémie Asselin,[†,‡] Neftaha Tazi,[†] Younès Messaddeq,[‡] Dennis Levinson,[§] and Ze Zhang[∥]

[†]Groupe de Recherche en Écologie Buccale, Faculté de Médecine Dentaire, Université Laval, 2420 Rue de la Terrasse, Québec, QC G1V 0A6, Canada

[‡]Département de Physique, Génie Physique et d'Optique, Faculté de Sciences et Génie, Université Laval, 2375 Rue de la Terrasse, Québec, QC G1V 0A6, Canada

[§]Department of Medicine, University of Illinois, Chicago, Illinois 60612, United States

[∥]Département de Chirurgie, Faculté de Médecine, Centre de Recherche de l'Hôpital Saint-François d'Assise, CHU, Université Laval, Québec, QC G1V 0A6, Canada

ABSTRACT: Bacterial cellulose (BC), a three-dimensional fibril, is a natural polymer that can be used for many applications. BC effectiveness may be improved by enhancing surface characteristics contributing to a better physiologic interaction with human and animal cells and to intrinsically present antimicrobial agents. In the present study, gentamicin-activated BC membranes were obtained by chemically grafting RGDC peptides (R: arginine; G: glycine; D: aspartic acid; C: cysteine) using coupling agent 3-aminopropyltriethoxysilane (APTES) followed by covalent attachment of gentamicin onto the surface of the BC membrane network. X-ray photoelectron spectroscopy (XPS) analyses showed that the BC−APTES contained 0.7% of silicon in terms of elemental composition, corresponding to a grafting ratio of 1:12. The presence of silicon and nitrogen in the BC−APTES confirmed the surface functionalization of the BC membrane. Fourier-transform infrared (FTIR) analyses show the formation of the secondary amide as supported by the valence bond C═O ($\nu_{C=O}$), a characteristic vibrational transition at 1650 cm^{-1} which is particularly intense with the BC−RGDC−gentamicin membrane. Energy-dispersive X-ray (EDX) analyses showed a low level of carbon and nitrogen (C + N) in pure BC but a high level of (C + N) in BC−RGDC−gentamicin confirming the surface modification of the BC membrane by RGDC and gentamicin enrichment. Of great interest, the gentamicin−RGDC-grafted BC membranes are bactericidal against *Streptococcus mutans* but nontoxic to human dermal fibroblasts and thus may be useful for multiple applications such as improved wound healing and drug delivery systems.

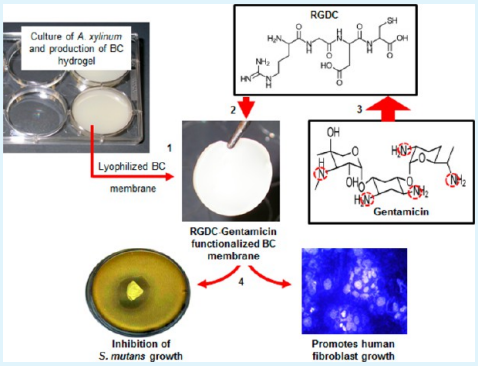

KEYWORDS: *bacterial cellulose, RGDC peptides, antimicrobial, gentamicin, gingival fibroblasts*

INTRODUCTION

Biopolymers are shown to be applicable to alimentary, biomedical, pharmaceutical, and biotechnological fields.[1−3] Cellulose, one of the most versatile polymers, consists of long linear chains of 1,4-β-D-glucopyranose linked by hydrogen bonds giving it a hard network.[4,5] Cellulose chain linearity yields multiple elementary fibrils that aggregate into larger bundles which contain crystalline and amorphous regions. Cellulose crystallinity is dependent on the origin of the cellulose and any physical or chemical modifications to which it was subjected.[6,7] Because of its widespread occurrence as well as uniform molecular structure and properties such as polyfunctionality, hydrophilicity, and biocompatibility, cellulose is of great importance in both fundamental and industrial research.[8−10] In addition to plants, bacteria such as *Acetobacter xylinum* are able to produce cellulose in the form of pellicles at the air/liquid interface of the culture medium in static culture.[11,12] Bacterial cellulose (BC) exhibits superior purity when compared with plant cellulose,[6] justifying its potential use in several applications. BC is a natural, biodegradable polymer with excellent mechanical properties.[13] It consists of elementary cellulose fibrils, whose diameter typically lies in the range of 3−40 nm.[14] As plant cellulose, BC fibers contain both crystalline and amorphous regions. The crystalline regions are responsible for the fibers' high tensile strength, while amorphous regions provide flexibility to the cellulose structures.[15,16] Chemically, native cellulose contains a large number of hydroxyl groups leading to the formation of hydrogen bonds which contribute to its interaction with diverse molecules and macromolecules of varying polarity.[4,5] The adsorption and adhesion phenomena depend on the organization of glucan chains located at the surface of the cellulose microfibrils.[17] As an example, the

Received: July 15, 2013
Accepted: January 7, 2014
Published: January 7, 2014

   dx.doi.org/10.1021/am4027983 | *ACS Appl. Mater. Interfaces* 2014, 6, 1439−1446

association of hydrophilic structures, including hydrocolloids such as xyloglucan, with cellulose can modify the mechanical and chemical properties of cellulose.[18]

Natural and synthetic polymer surface modification is a common functionalization and bioactivation process. The uses of small peptides show significant benefits when compared to coating polymer surfaces with matrix proteins such as fibronectin, which can be subjected to both enzymatic degradation and immune inactivation.[19,20] Use of the arginine-glycine-aspartic acid (RGD) sequence to functionalize polymer surfaces has been shown to contribute to cell adhesion, spreading, and wound healing.[21−24] Therefore, developing hybrid biomaterials equipped with such peptide sequences represents an attractive alternative to improve cell−biomaterial interactions. Surface-functionalized BC to generate hybrid polymers equipped with antimicrobial peptides is another important application as previously shown by incorporating aminoalkyl groups to the BC.[25] In recent years multiple interests were dedicated to studying BC production[11] and the development of new nanocomposite materials for various applications.[26,27] In the present study, the BC polymer was produced and functionalized by grafting arginine-glycine-aspartic acid-cysteine (RGDC) peptides and then enriching the polymer with an antimicrobial agent, gentamicin. RGDC-functionalized BC polymers with and without gentamicin were characterized in terms of chemical composition and morphology. Functionalized BC polymers were also evaluated for antimicrobial activity against *Streptococcus mutans* and the effect on cell adhesion and proliferation using human gingival fibroblasts.

MATERIALS AND METHODS

Production of BC Membranes. *Acetobacter xylinum* (ATCC 52582) obtained from the American Type Culture Collection (Rockville, MD) was cultivated in 12-well plates with 5 mL of culture medium per well for 6 days at 28 °C in static culture conditions. The nutrient medium contained 2 wt % glucose, 0.5 wt % peptone, 0.5 wt % yeast extract, 0.27 wt % disodium hydrogen phosphate, and 0.115 wt % citric acid. Bacterial cellulose pellicles were harvested and cleaned by immersion in 2 wt % NaOH solution at 80 °C for 1 h. The BC membranes were washed with deionized water and sterilized by autoclaving (121 °C for 15 min). Membranes were then frozen at −80 °C and lyophilized. The specimens were kept in a desiccator before analysis. The thickness of such membranes was estimated to 100−200 μm.

Surface Modification of the BC Membranes. The lyophilized cellulose membrane surface was covered with covalently bound silane chains. This was obtained by immersing the BC membranes in a solution of 0.4 M/L 3-aminopropyltriethoxysilane (APTES, Sigma-Aldrich, USA) in anhydrous toluene for 90 min with agitation under a nitrogen atmosphere. The BCs were then rinsed three times with 25 mL of anhydrous toluene under nitrogen atmosphere. Following the third wash, the APTES-grafted cellulosic materials were immersed in a solution of dimethylformamide (DMF) for 5 min and then transferred to a heterobifunctional cross-linker consisting of 2 mM/L of 3-succinimidyl-3-maleimidopropionate (SMP, TCI America, USA), 2 mM in DMF for 90 min under nitrogen atmosphere. After the reaction, BC membranes were washed three times with DMF then immersed in a 1 mM/L RGDC (Arg-Gly-Asp-Cys, GenScript, USA) solution in DMF. The contact of cellulosic membranes with RGDC−DMF solution was done overnight under light agitation. BC membranes were then washed two times with anhydrous DMF followed by three washes with distilled water and dried under sterile conditions.

X-ray Photoelectron Spectroscopy (XPS) Analysis of the Pure BC before and after APTES Treatment. The surface chemistry of the specimens was analyzed with a PerkinElmer PHI model 5600 X-ray photoelectron spectrometer (Chanhassen, MN, USA) for both a survey scan (aluminium X-ray source) to detect surface elemental composition and a high-resolution scan (magnesium X-ray source) on carbon and oxygen to detect surface functional groups. The take-off angle was at 45°. The spectra were analyzed using the software provided by the manufacturer.

Gentamicin Grafting onto Modified Cellulosic Membranes. RGDC-functionalized BC membranes were immersed in gentamicin sulfate solution (10 mg/mL, Fisher Scientific, Ottawa, ON, Canada) for either 24 h or 7 days. Gentamicin-grafted BC membranes were then extensively washed with sterile distilled water,and dried in a sterile atmosphere. Data presented in this manuscript are those obtained after 24 h of contact between the RGDC−BC-functionalized membrane and gentamicin.

Scanning Electron Microscopy (SEM) Analysis. Scaffolds (pure BC, BC−RGDC, and BC−RGDC impregnated with gentamicin solution) were subjected to SEM analyses. For this purpose, scaffold dehydration was performed in a series of ethanol solutions of increasing concentrations (50, 70, 90, and twice at 100%), with a 5 min dehydration treatment in each solution. The dehydrated specimens were kept overnight in a vacuum oven at 25 °C, after which they were sputtercoated with gold and examined with a JEOL 6360 LV SEM (Soquelec) operating at appropriate accelerating voltage. Photos were taken from the membrane surface and on membrane cross sections. These were used to determine the thickness of each type of membrane (n = 4).

Fourier Transform Infrared Spectroscopy (FTIR). Pure BC, BC−RGDC, and BC−RGDC−gentamicin membranes were analyzed on a Magna 850 FTIR spectrometer (Thermo Scientific, Madison, WI, USA) using a nitrogen-cooled MCT detector and OMNIC software. A Golden Gate accessory (Specac Ltd., London, U.K.) was used to press the samples up to 80 lbs on an ATR diamond. For each analysis, 128 scans were averaged per sample (n = 4) with a resolution of 4 cm^{-1}.

Energy-Dispersive X-ray Spectroscopy (EDX) Analysis. Pure BC, BC−RGDC, and BC−RGDC−gentamicin were subjected to EDX analyses. Dried specimens were sputter coated with Au−Pd, and the specimens were analyzed by means of EDX (Genesis XM2 Imaging 60 System-EDAX, USA). The experiment was repeated four times, and representative photographs were taken (n = 4).

Assay of Antimicrobial Activity. Antibacterial activity of the pure BC, BC−RGDC, and BC−RGDC−gentamicin membranes was determined against *S. mutans* (ATCC 25175) using a disc diffusion method. Initial cultures of *S. mutans* were grown at 37 °C in TYE medium containing (per liter) 10 g of tryptone (Difco Laboratories, Detroit, MI, USA), 2.5 g of NaCl, 2.5 g of $NaHPO_4$, and 0.5% (w/v) glucose until the optical density at 660 nm reached 0.4. The bacteria were then harvested by centrifugation, washed three times in TYE medium, and then adjusted to 10^6 cfu/mL. The bacterial suspension was used to overlay a 60 mm diameter Petri dish containing gelose agar. Subsequently, the different BC membrane (pure BC, BC−RGDC, BC−RGDC−gentamicin) discs (5 mm diameter) were placed on the bacteria-seeded agar surfaces (one disc per plate) and incubated at 37 °C for 24 h. The inhibition zone was photographed and estimated by measuring the diameter to the nearest whole millimeter. The experiment was repeated four times, and the average value was calculated (mean + SD).

Human Fibroblast Adhesion and Proliferation after Culture onto BC Membranes. Normal human skin fibroblasts (ScienCell Research Laboratories, Carlsbad, CA, USA) were cultured in Dulbecco's modified Eagle's (DME) medium supplemented with 10% fetal bovine serum (FBS). The medium was changed three times a week. When the culture reached 90% confluence, the cells were detached from the flasks with a 0.05% trypsin−0.1% EDTA solution, washed twice, and resuspended in FBS-supplemented DME medium. Cells were seeded (10^3 cells/cm^2) onto the different BC membranes. Cultures were maintained in a 5% CO_2 humid atmosphere at 37 °C for 24 and 48 h. At the end of each culture period, the cell-populated BC membranes were subjected to a MTT viability assay. Briefly, a stock solution (5 mg/mL) of MTT (tetrazolium dye) was prepared in PBS

and added to each culture well at a final concentration of 10% (v/v). The fibroblast-populated BC membranes were then incubated for 4 h at 37 °C with MTT. The supernatant was then removed, and BC membranes were washed once with warm PBS. After washing, the BC membranes were overlayed with 1 mL of 0.04 N HCl in isopropanol and incubated for 15 min under agitation. Finally, 200 μL (in triplicate) of the reaction mixture was transferred to a 96-well, flat-bottom plate, and absorbance was measured at 550 nm using an enzyme-linked immunosorbent assay (ELISA) reader (X-Mark microplate spectrophotometer, BioRad Laboratories, Mississauga, ON, Canada). To confirm the biocompatibility of the BC membranes we analyzed cell adhesion and density on each BC membrane by using Hoechst staining. To do so, following each culture period, specimens were washed and fixed with 25% glacial acetic acid in a methanol solution (v/v). Each well was then supplemented with 0.5 mL of Hoechst 33342 (H42) (Riedel de Haen, Seele, Germany) in PBS (1 mg/mL), and the specimens were incubated in a dark environment for 10 min at room temperature prior to being extensively washed with distilled water and observed under an epifluorescenc light microscope (Axiophot, Zeiss, Oberkochen, Germany). Results are reported as the mean ± SD of four separate experiments.

Statistical Analyses. Each experiment was performed four times, with experimental values expressed as the means ± SD. The statistical significance of the differences between the control (pure BC) and the experimental (gentamicin−RGDC-functionalized BC) values was determined with a one-way ANOVA. Posteriori comparisons were performed using Tukey's method. Normality and variance assumptions were verified using the Shapiro−Wilk test and the Brown and Forsythe test, respectively. All of the assumptions were fulfilled. *P* values were declared significant at ≤0.05. Data were analyzed using the SAS version 8.2 statistical package (SAS Institute Inc., Cary, NC, USA).

RESULTS AND DISCUSSION

On the basis of the fact that BC is a unique and promising material for use as a modified or unmodified structure for multiple applications, due to its composition[11] and its ability to be engineered structurally and chemically on nano-, micro-, and macroscales,[28,29] we optimized experimental conditions to engineer BC hydrogel as a three-dimensional thick membrane (Figure 1a). Following washing and lyophilization, the scaffold was subjected to SEM analysis. The unmodified BC membrane shows the expected nanofiber structure (Figure 1b). Due to its three-dimensional micro- and nanofibrillar structure, along with its inherent biocompatibility,[24] BC has generated considerable interest for use in different applications including tissue replacement, medical implants, drug delivery systems,[30] and wound healing.[31] The potential use of BC was encouraged by polymer functionalization with different molecules or chemical groups to impact BC interaction with mammalian cells[32] and also to improve antimicrobial strategies against infection.[25] For this purpose, we first activated the BC surface with the primary amine groups (−NH_2) in APTES (Figure 2) through the interaction of the hydroxyl (−OH) groups of the BC with the silicon atom on APTES. XPS data showed that the BC−APTES contained 0.7% of silicon in terms of elemental composition (Table 1). Because no silicon was detected in the original BC, the presence of silicon in the BC−APTES was attributed to the APTES grafted on BC fibers rather than to contamination. On the basis of the theoretical structure of BC that contains 11 atoms (5 oxygen and 6 carbon) in each repeat unit and the theoretical structure of the grafted and hydrolyzed APTES that contains 7 atoms (3 carbon, 2 oxygen, 1 silicon, and 1 nitrogen), this 0.7% of silicon corresponds to a grafting ration of 1:12, meaning every 12 repeat units in BC structure were grafted with 1 APTES (1/((11 × 12) + 7)) = 0.7%). While this is only an estimation because of the presence of other trace

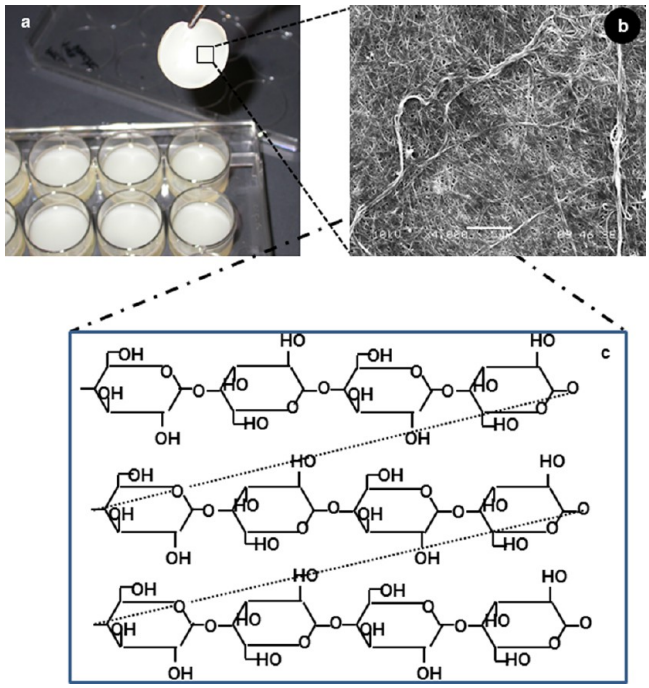

Figure 1. BC production and analyses: macroscopic observation of the BC materials (a), SEM image of the pure BC membrane (b, bar 2 μm), and chemical structure of cellulose (c).

elements and irregular structures in BC, the low grafting ratio was confirmed, and it also explained why no significant difference was detected between the ^{13}C NMR spectra of BC and BC−APTES (data not shown). The slightly lower oxygen content in the APTES grafted BC (39.2 in BC−APTES vs 43.2 in BC) also supports this low grafting ratio (APTES contains less oxygen than BC does). However, the presence of high nitrogen content (3.7%) relative to silicon content in the BC−APTES cannot be solely explained by the primary amine group in APTES (theoretical ratio of Si:N = 1 in APTES). The high-resolution spectrum of O_{1s} showed two peaks assigned to hydroxyl and ether groups. The slightly increased OH groups in BC−APTES support the grafting of APTES and the hydrolysis of the two CH_3CH_2−O−Si groups. The C_{1s} was assigned to hydrocarbons C<u>C</u>C, C<u>C</u>O, and O<u>C</u>O, and among them the C<u>C</u>C in BC is likely from contamination and the structures different from the theoretical chemical form of BC, which was also reported elsewhere.[33] We then produced the gentamicin-enriched BC membrane following grafting RGDC to the APTES on the BC membrane surface (Figure 2). These include the interactions of the hydroxyl (−OH) groups of the BC with the silicon atoms on APTES to create an activated BC surface enriched with amine groups (−NH_2). These amine groups can react with the ester (−COO) of the cross-linker SMP. Covalent binding of RGDC is possible through nucleophilic interaction of the thiol (−SH) of cysteine with the cross-linker. Gentamicin was then grafted to the BC−RGDC complex through available carboxylic acid (−COOH) on RGDC and the amine groups of the gentamicin. These different steps produce an antimicrobial active BC surface functionalized with RGDC and gentamicin. Similar work has previously been reported incorporating different molecules[34,35] into the 3D network of the BC to improve its antimicrobial role.

Functional Groups on the BC−RGDC−Gentamicin. The functional groups of different BC membranes were

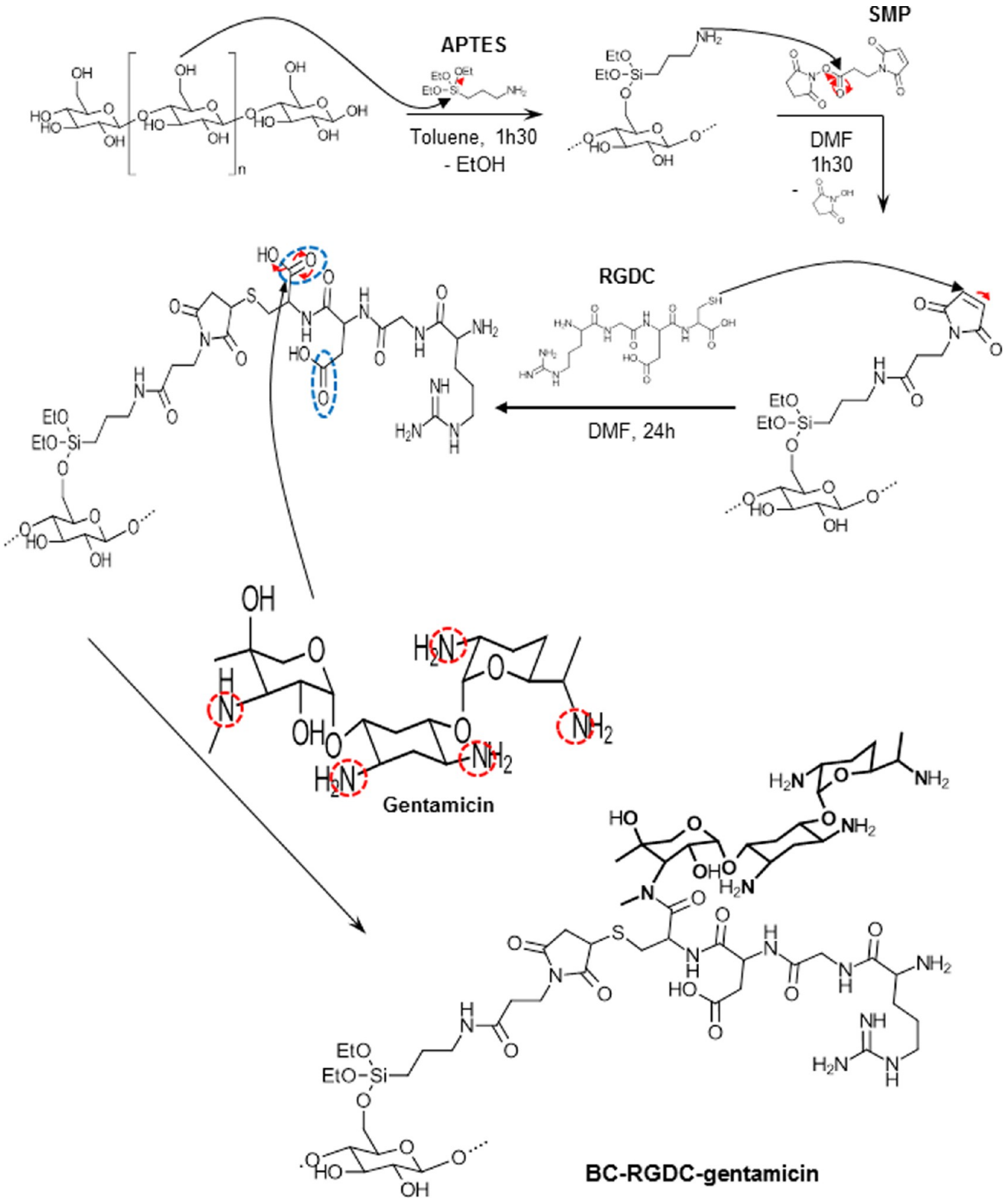

Figure 2. Chemical mechanism of BC membrane surface activation by grafting of RGDC and gentamicin. The covalent binding also requires 3-aminopropyltriethoxysilane (APTES) as an initiator and succinimidyl maleimidopropionate (SMP) for cross-linking.

analyzed using FTIR surface analyses, showing interesting differences between the different BC membranes. The complete spectra showed typical C−H vibrations near 2900 cm^{-1} and O−H vibrations near 3300 cm^{-1} that are common for BC (Figure 3I). Enlargement of the IR spectra between 1800 and 900 wavenumber/cm showed (Figure 3II) that the absorption at 1650 cm^{-1}, characteristic of amide I in peptide (C═O stretching), is observed for BC (C), BC−RGDC (B), and BC−RGDC−gentamicin (A). Because ideal BC does not contain a C═O group (Figure 1), the presence of the amide I in spectrum C is probably because of the contamination or irregular structures as detected by XPS (C_{1s}). The addition of

dx.doi.org/10.1021/am4027983 | ACS Appl. Mater. Interfaces 2014, 6, 1439−1446

Table 1. XPS Analysis of BC and BC−APTES Fibers

	surface elemental composition (%)							
samples	C	O	N	Si	Na	P	Cl	Ca
BC	50.2	43.2	0.7	-	4.4	0.9	0.4	0.2
BC−APTES	56.4	39.2	3.7	0.7	-	-	-	-
	surface chemical groups (%)							
	C−O−H	C−O−C	C−C−C	C−C−O	O−C−O			
BC	90.5	9.5	18.0	58.5	23.5			
BC-APTES	93.0	7.0	22.3	53.2	24.5			

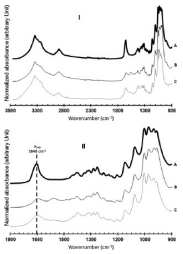

Figure 3. FTIR spectra of the different materials. (I) Complete IR spectra of each material; (II) enlarged IR spectra (1800−900). In panel (II), the FTIR spectra were normalized against the absorption at 1056 cm^{-1} for all modified membranes. A: BC−RGDC−gentamicin. B: BC−RGDC. C: Pure BC (n = 4).

RGDC is evidenced by the amide II at about 1560 cm^{-1} (Figure 3II, N−H bending + C−N stretching) that is stronger in spectrum B than that in spectrum C. The strongest amide I in the spectrum of BC−RGDC−gentamicin is because of the contribution of the primary amine groups in gentamicin (N−H bending). No absorption of C═O in carboxylic acid or in ester between 1700 and 1750 cm^{-1} was observed, likely because of the limited number of carboxylic acid groups in BC−RGDC. Similar data were reported with RGD-functionalized chitosan polymer showing an absorption band at 1474 cm^{-1} confirming the introduction of methyl groups on the chitosan backbone.[36] These data support our work showing the functionalization of BC through RGDC grafting groups. To further confirm this functionalization, we performed EDX analyses. Figure 4 shows a low level of carbon and nitrogen (C + N) with pure BC. This level is increased with BC−RGDC and BC−RGDC−gentamicin. The highest level of C + N is obtained with the RGDC-functionalized BC membrane that has been covalently enriched with gentamicin. This further confirms the surface modification of the BC membrane by RGDC and gentamicin enrichment.

Surface Morphology of the BC Membranes. The morphology of the pure BC-functionalized membranes was observed by SEM (Figure 5). The fibers show homogeneous shape with smooth surfaces (Figure 5a). The pure BC membrane showed a high density of pores spread over the surface of the BC membranes. Attachment of the RGDC peptide on the surface of the BC nanofibers and the effect of immersion of the membranes in apolar and low-polarity solvents decreases the apparent porosity on BC−RGDC (Figure 5b). It is also important to note that pores are still available over the surface of the BC−RGDC-functionalized membrane. These pores may facilitate scaffold colonization with cells when used as a cell growth vehicle. Both pure BC and BC−RGDC-functionalized membrane show a typical 3D network structure. These data are comparable to those obtained with BC functionalized with aminoalkyl groups.[25] Similarly,

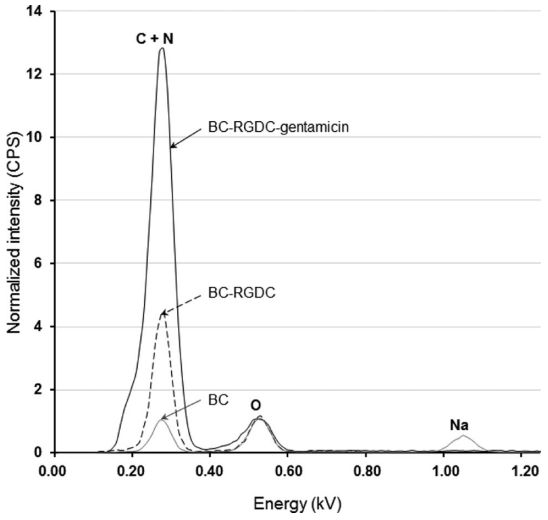

Figure 4. Energy-dispersive X-ray spectroscopy (EDX) analyses: BC and modified BC membranes were analyzed with EDX and presented (n = 4). Analyses showed increased total level of carbon and nitrogen (C + N) with the grafting of RDGC and gentamicin. C + N: total level of carbon and nitrogen. O: level of oxygen. Na: level of sodium.

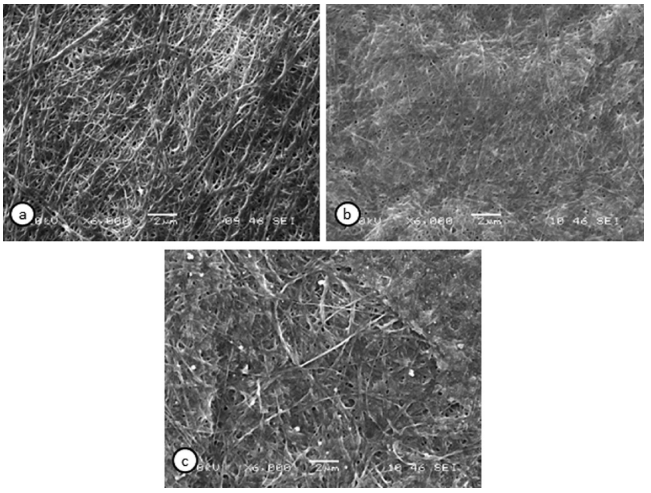

Figure 5. Scanning electron microscopy images. (a) Pure BC membrane, (b) BC−RGDC membrane, and (c) BC−RGDC−gentamicin membrane (scale bars, 2 μm).

bacterial cellulose functionalized with pectin showed nanofiber embedment and reduced pore density.[36] The next question is: what is the surface morphology of the BC when functionalized with RGDC and coupled to gentamicin? Figure 5c shows a similar morphological structure as the pure BC or the RGDC-functionalized BC, even though it still appears less porous than pure BC. These results are comparable to those reported by Saska et al.,[37] showing that osteogenic growth peptide incorporation into BC membranes did not change the morphology of the BC nanofiber and its crystalline pattern.[37] It is also important to note that even after RGDC−gentamicin fixation onto the surface of the BC membrane several pores are still available. Thus, the functionalization of the BC membrane by grafting RGDC−gentamicin does not lead to inappropriate surface modification of the BC membrane. The examination of the BC membrane cross-section confirmed that the increased membrane thickness is probably caused by the solvent DMF that can swell BC as seen in Figure 6. Such swelled structure

dx.doi.org/10.1021/am4027983 | ACS Appl. Mater. Interfaces 2014, 6, 1439−1446

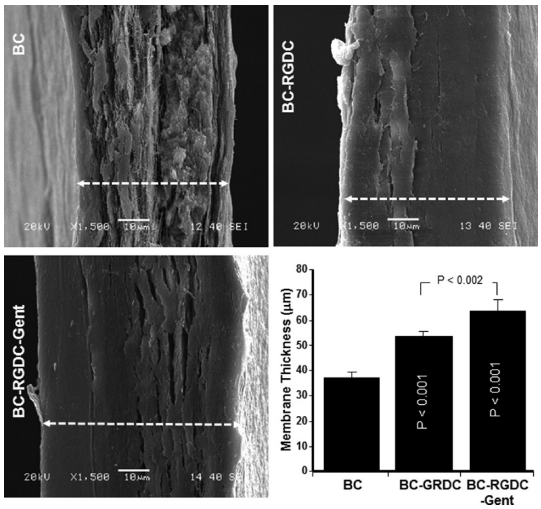

Figure 6. Thickness of the different BC membranes. Following surface functionalization or not, BC membranes were subjected to SEM analyses. Representative photos were presented. Thickness was determined using different cross sections from different membranes (n = 4).

also favors entrapment of RGDC peptides and gentamicin. Because SEM and FTIR analyses show changes at the surface and the thickness of functionalization of the BC membrane by RGDC−gentamicin grafting, it is important to confirm such results by investigating antimicrobial activity of the gentamicin-enriched BC membranes.

Bacterial Activity of Gentamicin−RGDC-Functionalized BC Membrane. The effect on bacterial growth of the grafted gentamicin on BC nanofibrils was assessed by inoculating BC membranes with *S. mutans* bacteria. As shown in Figure 7, the pure BC membrane (Figure 7a) and RGDC-functionalized BC membrane (Figure 7c) have no effect on bacterial growth. However, BC−RGDC−gentamicin shows a significant reduction in bacterial growth after 24 h (Figure 7d). These observations were confirmed by measuring the inhibition zone of bacterial growth on gelose agar (Figure 8). No growth inhibition was noted with either pure BC or RGDC-functionalized BC membranes. Gentamicin grafted to BC through RGDC peptide linkage shows significant growth inhibition as ascertained by diameter size measured on gelose agar. Thus, the bactericidal activity of the functionalized BC membrane is due to the introduction of gentamicin onto the BC nanofibrils. Our data are comparable to those BC membranes functionalized with aminoalkyl groups.[25] Overall, these data demonstrate the ability to improve the bactericidal activity of the BC membrane by grafting an antibacterial agent onto the cellulose nanofibers through RGDC linking. Since RGD−peptide interactions are possible with a variety of proteins, other agents could possibly be grafted onto functionalized BC surfaces. Such BC membranes could be useful to control tissue infection. When used for such applications, a functionalized BC membrane will also be in contact with human cells raising the concern of BC biocompatibility.

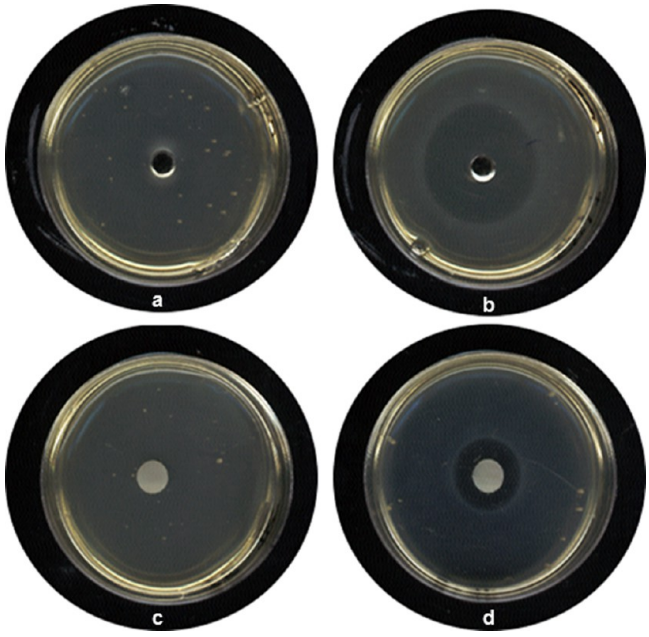

Figure 7. Efficacy of gentamicin−RGDC-grafted BC against *S. mutans* growth: representative photos of the inhibition zone of the gentamicin−BC membrane against *S. mutans* growth following 24 h incubation at 37 °C. (a) Pure BC, (b) pure gentamicin; (c) RGDC−BC; and (d) BC−RGDC−gentamicin (n = 4).

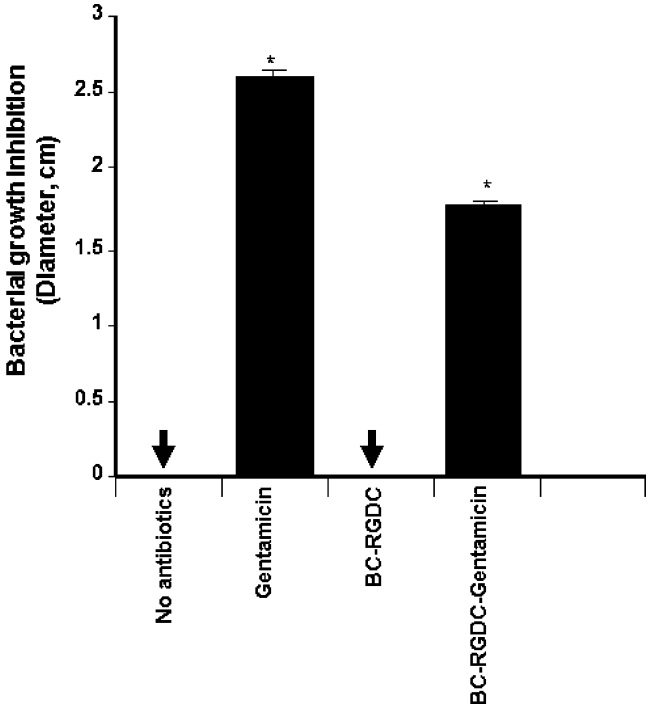

Figure 8. Measurement of the inhibition zone diameter of gentamicin bioactivated BC membranes. *: $P < 0.01$ when comparing the pure BC membrane to the gentamicin−RGDC-functionalized membrane (n = 4).

Effect of the Functionalized BC Membrane on Human Fibroblast Adhesion/Growth. The effect of the functionalized BC membrane network on the adhesion and proliferation of human skin fibroblasts was investigated. Previously, multiple cell lines have been used to investigate the biocompatibility of polymers based on bacterial cellulose.[24,38,39] As expected, pure BC membranes were nontoxic to human fibroblasts (Figure 9). Furthermore, when adding RGDC to BC membranes, we see a significant increase of fibroblast number at 24 and 48 h. Since

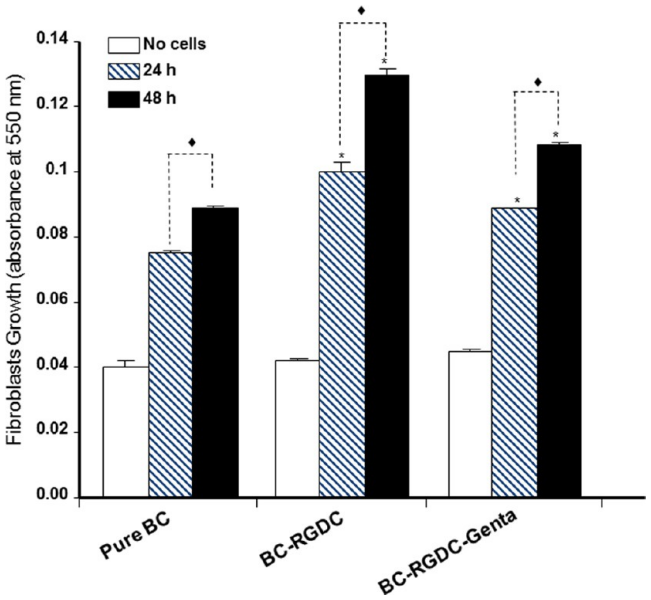

Figure 9. Biocompatibility of gentamicin−RGDC−BC membranes: Human dermal fibroblast proliferation on contact with BC and BC-functionalized membranes after 24 and 48 h culture. Data are presented as mean ± standard deviation ($n = 4$). (*) refers to $p < 0.01$ when comparing to controls (fibroblast seeded pure BC). (♦) refers to $p < 0.01$ when comparing 24 to 48 h.

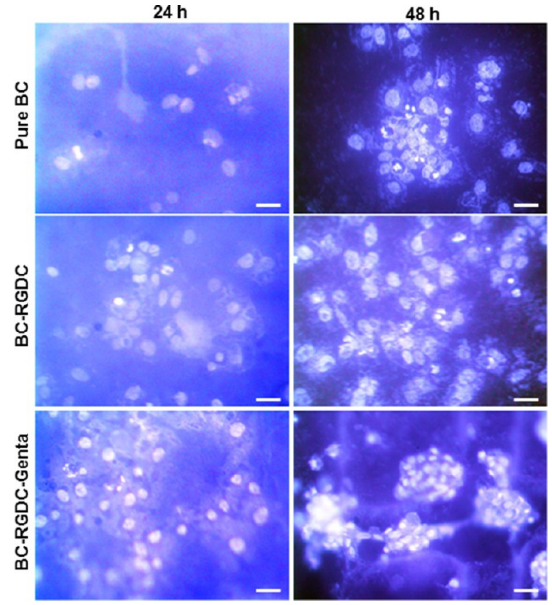

Figure 10. Visualization of fibroblast adhesion and growth onto BC-functionalized membranes. Cells were seeded onto different BC polymers and cultured for 24 or 48 h. Membranes were then were subjected to Hoechst staining. Representative photos were presented (scale bars, 50 μm).

peptides such as RGDC were identified as mediating the attachment of cells to several plasma and ECM proteins including fibronectin, vitronectin, and laminin,[19,40] multiple initiatives have been used to deposit RGD-containing peptides on the surface of different biomaterials improving mammalian cell adhesion and growth.[19,41] Through this surface modification it is possible to add new properties to an identified polymer by integrating antimicrobial peptides or cell growth promoting factors.[42,43] In the present study, after BC surface functionalization with RGDC grafting groups, we incorporated gentamicin, showing the usefulness of such surface modification to control bacterial growth. We also tested the biocompatibility of such a membrane, showing the possibility of culturing human fibroblasts on the BC-functionalized membrane without observing any toxic effect. It is interesting to note that the surface-modified BC membrane with and without gentamicin significantly ($p < 0.01$) promotes fibroblast adhesion and growth as compared to nonfunctionalized BC membranes (Figure 9). These results were supported by the Hoechst staining. As shown in Figure 10, cells were spread out on the surface of each tested BC membrane. The cell density was higher after 48 h culture as compared to 24 h culture. It was also noted that the RGDC-functionalized BC membrane promotes cell adhesion and growth as compared to pure BC. These data confirmed those obtained with MTT assay. A similar observation was reported after BC functionalization with aminoalkyl groups.[25] In vivo studies showed that surface modification and gentamicin grafting onto hydroxyapatite material showed bone regeneration and limited tissue infection confirming the usefulness of antibiotic grafting through RGD groups onto the surface of polymers such as BC.[44]

CONCLUSION

In this study, BC−nanofiber membranes were produced and functionalized by introducing RGDC groups and further modified by introducing gentamicin onto the surface. XPS, FTIR, EDX, and SEM analyses confirmed the surface functionalization showing the presence of RGDC groups and gentamicin. The bactericidal activity of the RGDC−gentamicin-modified BC membrane was demonstrated by inhibiting the growth of *S. mutans*. The designed BC membrane was biocompatible, allowing human fibroblast growth. This biocompatibility was further enhanced by surface modification. This novel BC−RGDC−gentamicin membrane can therefore be seen as an effective antimicrobial candidate for multiple applications such as wound healing and drug delivery systems.

AUTHOR INFORMATION

Corresponding Author

*E-mail: mahmoud.rouabhia@fmd.ulaval.ca.

Author Contributions

All authors contributed to the experimental design and data analyses. The manuscript was written through contributions of all authors. All authors have given approval to the final version of the manuscript.

Notes

The authors declare no competing financial interest.

ACKNOWLEDGMENTS

Authors would like to acknowledge The Canada Excellence Research Chair (CERC-Chaire d'excellence en recherche du Canada sur l'innovation en photonique dans le domaine de l'information et des communications) and the NSERCs Discovery Program for the financial support (M.R. and Z.Z.).

REFERENCES

(1) Durango, A. M.; Soares, N.F.; Andrade, N. J. *Food Control* **2006**, *17*, 336−641.
(2) Nge, T. T.; Nogi, M.; Yano, H.; Sugiyama, J. *Cellulose* **2010**, *17*, 349−363.

(3) Czaja, W. K.; Young, D. J.; Kawecki, M.; Brown, R. M., Jr. *Biomacromolecules* **2007**, *8*, 1−12.
(4) Xu, F.; Shi, Y. C.; Wang, D. *Carbohydr. Polym.* **2013**, *94*, 904−917.
(5) Klemm, D.; Heublein, B.; Fink, H. P.; Bohn, A. *Angew Chem., Int. Ed Engl.* **2005**, *44*, 3358−3393.
(6) Guo, J.; Catchmark, J. M. *Carbohydr. Polym.* **2012**, *87*, 1026−1037.
(7) Tischer, P. C.; Sierakowski, M. R.; Westfahl, H., Jr.; Tischer, C. A. *Biomacromolecules* **2010**, *11*, 1217−1224.
(8) Brinchi, L.; Cotana, F.; Fortunati, E.; Kenny, J. M. *Carbohydr. Polym.* **2013**, *94*, 154−169.
(9) Fu, L.; Chen, S.; Yi, J.; Hou, Z. *Food Sci. Technol. Int.* **2013**, *0*, 1−11.
(10) Lavoine, N.; Desloges, I.; Dufresne, A.; Bras, J. *Carbohydr. Polym.* **2012**, *90*, 735−764.
(11) Petersen, N.; Gatenholm, P. *Appl. Microbiol. Biotechnol.* **2011**, *91*, 1277−1286.
(12) Fu, L.; Zhang, J.; Yang, G. *Carbohydr. Polym.* **2013**, *92*, 1432−1442.
(13) Siro, I.; Plackett, D. *Cellulose* **2010**, *17*, 459−494.
(14) Svagan, A. J.; Samir, M. A.; Berglund, L. A. *Biomacromolecules* **2007**, *8*, 2556−2563.
(15) Zimmermann, T.; Bordeanu, N.; Strub, E. *Carbohydr. Polym.* **2010**, *79*, 1086−1093.
(16) Henriksson, M.; Henriksson, G.; Berglund, L. A.; Lindstrom, T. *Eur. Polym. J.* **2007**, *43*, 3434−3441.
(17) Mazeau, K. *Carbohydr. Polym.* **2011**, *84*, 524−532.
(18) Zhou, Q.; Rutland, M. W.; Teeri, T. T.; Brumer, H. *Cellulose* **2007**, *14*, 625−641.
(19) Hersel, U.; Dahmen, C.; Kessler, H. *Biomaterials* **2003**, *24*, 4385−4415.
(20) Langer, R. *Acc. Chem. Res.* **2000**, *33*, 94−101.
(21) Aucoin, L.; Griffith, C. M.; Pleizier, G.; Deslandes, Y.; Sheardown, H. *J. Biomater. Sci. Polym. Ed.* **2002**, *13*, 447−462.
(22) Verrier, S.; Pallu, S.; Bareille, R.; Jonczyk, A.; Meyer, J.; Dard, M.; Amédée, J. *Biomaterials* **2002**, *23*, 585−596.
(23) Andrade, F. K.; Moreira, S. M.; Domingues, L.; Gama, F. M. *J. Biomed. Mater. Res., Part A* **2010**, *92* (1), 9−17.
(24) Pértile, R.; Moreira, S.; Andrade, F.; Domingues, L.; Gama, M. *Biotechnol. Prog.* **2012**, *28*, 526−532.
(25) Fernandes, S. C.; Sadocco, P.; Alonso-Varona, A.; Palomares, T.; Eceiza, A.; Silvestre, A. J.; Mondragon, I.; Freire, C. S. *ACS Appl. Mater. Interfaces* **2013**, *5*, 3290−3297.
(26) Lacerda, P. S.; Barros-Timmons, A. M.; Freire, C. S.; Silvestre, A. J.; Neto, C.P. *Biomacromolecules* **2013**, *14*, 2063−2073.
(27) Pinto, R. J.; Marques, P. A.; Neto, C. P.; Trindade, T.; Daina, S.; Sadocco, P. *Acta. Biomater.* **2009**, *5*, 2279−89.
(28) Lee, K. Y.; Tammelin, T.; Schulfter, K.; Kiiskinen, H.; Samela, J.; Bismarck, A. *ACS Appl. Mater. Interfaces* **2012**, *4*, 4078−4086.
(29) Chen, L. F.; Huang, Z. H.; Liang, H. W.; Guan, Q. F.; Yu, S. H. *Adv. Mater.* **2013**, DOI: 10.1002/adma.201204949.
(30) Valo, H.; Arola, S.; Laaksonen, P.; Torkkeli, M.; Peltonen, L.; Linder, M. B.; Serimaa, R.; Kuga, S.; Hirvonen, J.; Laaksonen, T. *Eur. J. Pharm. Sci.* **2013**, DOI: 10.1016/j.ejps.2013.02.023.
(31) Albaugh, K. W.; Biely, S. A.; Cavorsi, J. P. *Ostomy Wound Manage.* **2013**, *59*, 34−44.
(32) Fink, H.; Ahrenstedt, L.; Bodin, A.; Brumer, H.; Gatenholm, P.; Krettek, A.; Risberg, B. *J. Tissue Eng. Regener. Med.* **2011**, *5*, 454−463.
(33) Renata, A. N. P.; Fábia, K. A.; Clodomiro, A., Jr.; Miguel, G. *Carbohydr. Polym.* **2010**, *82*, 692−698.
(34) Luan, J.; Wu, J.; Zheng, Y.; Song, W.; Wang, G.; Guo, J.; Ding, X. *Biomed. Mater.* **2012**, *7*, 065006.
(35) Feese, E.; Sadeghifar, H.; Gracz, H. S.; Argyropoulos, D. S.; Ghiladi, R. A. *Biomacromolecules* **2011**, *12*, 3528−3539.
(36) Chen, X. G.; Park, H. J. *Carbohydr. Polym.* **2003**, *53*, 355−359.
(37) Saska, S.; Scarel-Caminaga, R. M.; Teixeira, L. N.; Franchi, L. P.; Dos Santos, R. A.; Gaspar, A. M.; de Oliveira, P. T.; Rosa, A. L.; Takahashi, C. S.; Messaddeq, Y.; Ribeiro, S. J.; Marchetto, R. *J. Mater. Sci. Mater. Med.* **2012**, *23*, 2253−2266.
(38) Dugan, J. M.; Gough, J. E.; Eichhorn, S. J. *Nanomedicine* **2013**, *8*, 287−298.
(39) Tazi, N.; Zhang, Z.; Messaddeq, Y.; Almeida-Lopes, L.; Zanardi, L. M.; Levinson, D.; Rouabhia, M. *AMB Express* **2012**, *2*, 61.
(40) Barczyk, M.; Carracedo, S.; Gullberg, D. *Cell Tissue Res.* **2010**, *339*, 269−280.
(41) Vidal, G.; Blanchi, T.; Mieszawska, A.; Calabrese, R.; Rossi, C.; Vigneron, P.; Duval, J. L.; Kaplan, D. L.; Egles, C. *Acta Biomater.* **2013**, *9*, 4935−4943.
(42) Drevelle, O.; Daviau, A.; Lauzon, M. A.; Faucheux, N. *Biomaterials* **2013**, *34*, 1051−1062.
(43) Monk, B. C.; Harding, D. R. *BioDrugs* **2005**, *19*, 261−278.
(44) Alt, V.; Bitschnau, A.; Böhner, F.; Heerich, K. E.; Magesin, E.; Sewing, A.; Pavlidis, T.; Szalay, G.; Heiss, C.; Thormann, U.; Hartmann, S.; Pabst, W.; Wenisch, S.; Schnettler, R. *Acta Biomater.* **2011**, *7*, 1274−1280.